JOURNAL OF SOLID STATE CHEMISTRY 84, 118–129 (1990)

Structure, Electrical Transport, and Magnetic Properties of the Misfit Layer Compound $(PbS)_{1.13}TaS_2$

J. WULFF, A. MEETSMA, S. VAN SMAALEN, R. J. HAANGE, J. L. DE BOER, AND G. A. WIEGERS*

Laboratory of Inorganic Chemistry, Materials Science Centre of the University, Nijenborgh 16, 9747 AG Groningen, The Netherlands

Received February 10, 1989; in revised form August 21, 1989

$(PbS)_{1.13}TaS_2$, formerly designated "$PbTaS_3$," has been found by single-crystal X-ray diffraction to be a misfit layer compound characterized by two face-centered orthorhombic unit cells each with space group $Fm2m$. One belongs to the PbS part of the structure (a = 5.825 Å, b = 5.779 Å, c = 23.96 Å, Z = 8), the other belongs to the TaS_2 part of the structure (a' = 3.304 Å, b' = 5.779 Å, c' = 23.96 Å, Z = 4). The corresponding axes are parallel; the ratio of the lengths of the misfit a axes, a/a' is irrational, but close to $\frac{7}{4}$. The compound is built of alternately double layers of PbS with distorted NaCl-type structure and TaS_2 sandwiches, with Ta in distorted trigonal prisms of sulfur. Along the c axes of length 23.96 Å, four units are stacked; units of the same type but $(\frac{1}{2})c$ apart are displaced with respect to each other over $(\frac{1}{2})b$. The symmetry of the complete structure is analyzed in terms of a four-dimensional superspace group. The electrical transport and magnetic properties are related to those of 2H–TaS_2. The conduction is metallic and strongly anisotropic, the in-plane resistivity being about 10^5 smaller than the resistivity along the c axis. The Hall coefficient, with positive sign, corresponds with an electron donation from PbS to TaS_2. The Seebeck coefficient is negative like that in other intercalates of 2H–TaS_2. The compound is Pauli-paramagnetic.

Introduction

Recent structural investigations (*1–6*) have shown that compounds formerly (*7–10*) designated as 1-1-3 chalcogenides MTS_3 (M = Sn, Pb, La; T = Nb) are misfit layer compounds built of alternately double layers of MS with distorted NaCl structure and NbS_2 sandwiches, with niobium in trigonal prisms of sulfur like Nb in 2H–NbS_2. Since slabs of MS and NbS_2 sandwiches have different geometries they do not form a compound with a single unit cell and space group; each compound MTS_3 is characterized by two-centered orthorhombic unit cells and two space groups. The c axes of the two structural units (MS and NbS_2) are perpendicular to the layers; they are equal in length or one is twice the other. The unit cells match along the b axes; the length of the b axes corresponds for the MS part with the cell edge of NaCl type MS (M = Sn, Pb, La) and for the NbS_2 part with $a\sqrt{3}$ of the unit cell of 2H–NbS_2 (a = 3.324 Å). In the direction perpendicular to the b and c axes, the lattices do not match; the length of the a axis of the MS part is approximately equal to the cell edge of the NaCl-type MS, while the a axis of the NbS_2 part is approximately equal to the a axis of 2H–NbS_2. The composition of these so-

* To whom correspondence should be addressed.

0022-4596/90 $3.00

called composite crystals is determined by the ratio a/a' and by the number of units MS and NbS_2 in each unit cell. The simplest structure is found for $(SnS)_{1.17}NbS_2$; along the direction of the c axes of length 11.761 Å, one slab of SnS and one sandwich of NbS_2 are present, the space groups being $Cm2a$ and $Cm2m$, respectively. For $(PbS)_{1.14}NbS_2$ and $(LaS)_{1.14}NbS_2$ the length of the c axis of the NbS_2 part of the structure is twice that of the PbS and LaS parts. The two NbS_2 sandwiches in $(LaS)_{1.14}NbS_2$ are related by a displacement of $(\frac{1}{2})b$; in this way the NbS_2 lattice is F-centered orthorhombic while the LaS lattice is C-centered.

In this paper we report the structure and some physical properties of "$PbTaS_3$," which turned out to be a misfit layer compound built of double layers of PbS and TaS_2 sandwiches, with Ta in distorted trigonal prisms of sulfur; the composition is $(PbS)_{1.13}TaS_2$.

Experimental

The compound was prepared by heating the elements in evacuated quartz ampoules at 850°C. Crystals were grown by vapor transport in a gradient of 930–850°C. To about 300 mg compound to be transported 5–10 mg $(NH_4)_2PbCl_6$, which acts as a convenient source for chlorine, was added. $(NH_4)_2PbCl_6$ decomposes at higher temperatures into $PbCl_2$, NH_4Cl, and Cl_2. The crystals grow at the low-temperature side of the tube as thin platelets.

The in-plane resistivity ($\rho_\perp$) and Hall coefficient (R_H) were measured on crystal platelets cut into a rectangular shape. Contacts, four and five for the in-plane resistivity and Hall effect, respectively, and two for the resistivity along the c axis were made with platinum paste. Resistivity versus temperature scans were performed with the sample in a liquid helium cryostate from 4 K to about 400 K using an ac current source (81 Hz) and a lock-in amplifier. Temperature setting and measurement of the resistance during the temperature scan were microcomputer controlled.

The Hall coefficient was determined in the temperature range 4–300 K with the field (from a superconducting magnet, Oxford Instruments) along the c axis of the crystal. An ac current source (81 Hz) was used; the Hall voltage was measured using a lock-in amplifier for fields from −3 to +3 T in steps of 0.5 T; plots of the Hall voltage versus field were made in order to check the linearity. The Hall voltage per unit field was determined by a least-squares fit to these points. Control and data handling were performed using a microcomputer.

The Seebeck coefficient from a powder compact was scanned automatically from 4 K to 300 K using a microcomputer for control of the temperature, temperature gradient, and the measurement of the thermo EMF; the Seebeck coefficient was determined by a least-squares fit to the EMF versus gradient data.

The magnetic susceptibility (χ) was measured in the temperature range 4–300 K using a Faraday balance (Oxford Instruments). Measurements were performed with powder compacts; since these compacts show a strong preferred orientation, magnetic measurements were performed with the magnetic field parallel and perpendicular to the axis of preferred orientation (c axis). We consider the measured χ values to be good estimates of $\chi_\parallel$ and $\chi_\perp$ for the field parallel and perpendicular the c axis.

Determination of the Structure of $(PbS)_{1.13}TaS_2$

Weissenberg photographs of a single crystal aligned along the common axis of 5.77 Å showed reflections due to two face-centered orthorhombic unit cells. Accurate unit cell constants obtained by least-squares from Guinier data (Jungner Instru-

ments, Cu$K\alpha_1$ radiation) are given in Table I; it is seen that the ratio $a/a' = 1.7555$ (SD 0.0009) is irrational but close to $\frac{7}{4} = 1.75$. Measurements using a CAD-4F single-crystal diffractometer (Enraf–Nonius) confirmed the indexing from Weissenberg and Guinier photographs. It may be remarked that the a axis of the PbS part from a single crystal is significantly smaller than a from powdered crystals (Table I). It is possible that the lattice parameters differ due to the mechanical treatment of the powder sample. Electron diffraction (*11*) also showed weak extra reflections (satellites) due to the mutual modulation of the TaS_2 and the PbS part of the structure. They occur on rows of the main spots parallel the a^* axes at positions with a component along these axes given by $r^* = h/a + n/a'$, for the modulated PbS lattice and by $r^* = h'/a' + n/a$ for the modulated TaS_2 lattice, n being the order of the satellite and h and h' the indices of reflections of the two subunits, respectively. The resulting diffraction pattern of satellites suggests therefore a unit cell with $a'' \approx 4a \approx 7a'$ for the whole structure.

From a comparison of the unit cells with the unit cells of $(SnS)_{1.17}NbS_2$ and $(PbS)_{1.14}NbS_2$, it is obvious that the structures are closely related. The face centering of both lattices PbS and TaS_2 in "$PbTaS_3$" implies that in each plane a C-centering is active while similar units $(\frac{1}{2})c$ apart are related by a displacement of $(\frac{1}{2})b$. From the ratio of the lengths of the a axes of the two structural units and the number of units PbS and TaS_2 per cell, 8 and 4 respectively, one calculates a composition of $(PbS)_{1.13}TaS_2$.

TABLE I

UNIT CELL DIMENSIONS AND SPACE GROUPS (SG) OF THE SUBLATTICES (SL)

	SL	a(Å)	b(Å)	c(Å)	SG
	PbS	5.8032(5)	5.7717(4)	24.002(2)	$Fm2m^a$
		5.825(1)	5.778(1)	23.962(2)	$Fm2m^b$
$(PbS)_{1.13}TaS_2$					
	TaS_2	3.3058(6)	5.7721(8)	24.002(5)	$Fm2m^a$
		3.3044(4)	5.779(4)	23.954(4)	$Fm2m^b$

[a] Measurements from a Guinier–Hagg camera.
[b] From a CAD-4F diffractometer.

Structure Refinement

Crystal data and experimental details of the refinements using reflection data from the PbS, TaS_2, and the common part of the diffraction pattern are compiled in Table IIa–IIc, respectively. The intensity data were corrected for scale variation (*12*), Lorentz and polarization effects, and absorption using a Gaussian integration method (*13*). The refinements were performed on F by full-matrix least-squares with unique reflections satisfying the $I \geq 2.5\,\sigma(I)$ criterion of observability. A refinement of the PbS data set (excluding $0kl$ reflections) with Pb and S at positions 8*c* of *Fm2m* converged to a R_F of 0.11; a difference Fourier synthesis revealed a rather large density at 0.8 Å from Pb along the Pb–S bond parallel c. We found a similar phenomenon during the refinement of the SnS part of $(SnS)_{1.17}NbS_2$; it was at that time not explained but we now suppose the occupance of such an "inverted" site in both cases to correspond with a Pb (Sn) atom "pushed" inside the double layer; in the normal case Pb (Sn) stick out of the planes of sulfur for about 0.4 Å. The origin of the occurrence of such a defect site is not clear; it is possible that it is connected to a sulfur deficiency, the apex S atom being not present in that case. It may be remarked that such a defect site was not found in the case of $(PbS)_{1.14}NbS_2$ (*5*). Refinements were performed with Pb randomly distributed over the two sites, viz. Pb(1), the regular site, and Pb(2), the site in the disordered lattice (Table III); the sum of the occupancy factor of both sites was constrained to 1.0. The refinement proceeded to $R_F = 0.074$ with about 10% of the Pb atoms in the disordered position.

TABLE IIa

X-RAY DATA COLLECTION OF $(PbS)_{1.13}TaS_2$

	PbS part	TaS_2 part
Diffractometer	Enraf–Nonius CAD-4F	
Radiation (Å)	Mo$K\bar{\alpha}$, 0.71073	
Monochromator	Graphite	
Temperature (K)	298	
Range; min. max., (deg)	1.7, 40.0	
$\omega/2\theta$ scan, (deg)	$\Delta\omega = 0.95 + 0.35$ tg θ	
Data set	h: 0 → 10; k: 0 → 10; l: −42 → 42	h: 0 → 5; k: 0 → 10; l: −42 → 42
Crystal-to-receiving-aperture distance (mm)	173	173
Horizontal vertical aperture (mm)	4.0, 4.5	4.0, 4.5
Reference reflections, r.m.s. dev. in %	0, 0, 16; 0.76 028; 1.21 $02\bar{8}$; 0.86	0, 0, 16, 1.21 028, 0.77 $02\bar{8}$, 0.98
Instability constant (P)	0.0105	0.0119
Drift correction	1.00–1.002	0.998–1.000
Min. and max. absorption correction fac.	1.31–19.17	1.31–15.26
X-ray exposure time (h)	21.7	7.8
Total data	1448	844
Unique data	738	429
Observed data ($I \geq 2.5\,\sigma(I)$)	534	428

The TaS_2 reflections excluding $0kl$ refined smoothly to $R_F = 0.033$ with the atoms on special positions 4*a* and 8*c* of *Fm*2*m* for Ta and S, respectively.

The complete structure was found from the $0kl$ reflections. Since these reflections occur only for k and l even, the b and c axes can be halved. The symmetry of the projected structure is that of the two-dimensional group *Pm*. For refinement using XTAL a three-dimensional space group had to be chosen; we chose *P*11*m* with the atoms on positions 1*a* and 2*c*. Refinements were performed with rigid TaS_2 and PbS units. The y of S was chosen as zero, y of Ta following from the TaS_2 refinement; z of Ta and S were also fixed at their values from the TaS_2 refinement, taking into account the difference in lengths of the b and c axes in both cases. The s.o.f. of the PbS

TABLE IIb

DETAILS OF THE REFINEMENT PROCEDURE OF $(PbS)_{1.13}TaS_2$

	PbS part	TaS_2 part
Number of reflections: $h \neq 0$	431	327
Number of refined parameters	19	10
Final agreement factors:		
$R_F = \Sigma(\|\|F_o\| - \|F_c\|\|)/\Sigma\|F_o\|$	0.074	0.033
$wR = [\Sigma(w(\|F_o\| - \|F_c\|)^2)/\Sigma w\|F_o\|^2]^{1/2}$	0.055	0.041
Weighting scheme	$1/\sigma^2(F)$	$1/\sigma^2(F)$
$S = [\Sigma w(\|F_o\| - \|F_c\|)^2/(m-n)]^{1/2}$ m = number of observations n = number of variables	3.838	3.375
Min. and max. residual densities in final difference Fourier map (e/Å^3)	−10.5, 5.1	−3.20, 5.16
Max. (shift/sigma) final cycle	0.018	0.087
Average (shift/sigma) final cycle	0.0031	0.003

TABLE IIc

REFINEMENT OF THE PROJECTION ALONG [100]

Refinement in space group *P*11*m* (No. 6) b = 2.889(1) Å, c = 11.891(2) Å

Number of reflections: $h = 0$	101
Number of refined parameters	15
Final agreement factors:	
$R_F = \Sigma(\|\|F_o\| - \|F_c\|\|)/\Sigma\|F_o\|$	0.056
$wR = [\Sigma(w(\|F_o\| - \|F_c\|)^2)/\Sigma w\|F_o\|^2]^{1/2}$	0.065
Weighting scheme	1
$S = [\Sigma w(\|F_o\| - \|F_c\|)^2/(m-n)]^{1/2}$ m = number of observations n = number of variables	3.122
Residual electron density in final difference Fourier map (e/Å^3)	−0.75, 1.17
Max. (shift/sigma) final cycle	0.0137
Average (shift/sigma) final cycle	0.0045

TABLE III

FINAL FRACTIONAL ATOMIC COORDINATES AND TEMPERATURE FACTORS, WITH THEIR E.S.D. VALUES IN PARENTHESES, OF $(PbS)_{1.13}TaS_2$

	x	y	z	s.o.f.	U_{eq}(Å^2)[a]
(a) PbS					
Pb(1)	0.0	0.0	0.31847(6)	0.896(6)	0.0303(4)
Pb(2)	0.0	0.514(9)	0.2167(5)	0.102(6)	0.043(6)
S(1)	0.0	0.018(6)	0.2007(4)	1.0(0)	0.045(3)
(b) TaS_2					
Ta(1)	0.0	0.0	0.0		0.0067(1)
S(1)	0.0	0.3438(7)	0.0650(1)		0.0080(8)
Common part[b]					
Pb(1)	—	0.517(2)	0.6366(5)	0.52(1)	0.0225(1)
S(1)	—	0.553(2)	0.4011(5)	0.52(1)	0.0305(1)
Ta(1)	—	0.6877(0)	0.0	1.0(0)	0.0053(1)
S(2)	—	0.0	0.1300(0)	1.0(0)	0.0087(1)

[a] $U_{eq} = \frac{1}{3}\Sigma_i\Sigma_j U_{ij} a_i a_j \mathbf{a}_i \cdot \mathbf{a}_j$.

[b] Coordinates in a unit cell with b = 2.889(1) Å, c = 11.981(2) Å.

unit and its y and z coordinates were refined, and converged to $R_F = 0.056$. The z coordinates are with e.s.d. equal to those found from the "PbS" refinement. The disorder in the Pb sublattice as found from the PbS refinement was not taken into account. The s.o.f. of the PbS unit (0.52(1)) is somewhat lower than expected from the ratio of the a axes, 0.565, respectively. The temperature factors of PbS and TaS_2 in the projected structure follow the trend already visible in the separate refinements, viz., those of PbS being about five times larger than those of TaS_2. It may be remarked that it is now, at this stage of the structure determination, possible to change the y coordinates of the atoms in the PbS and TaS_2 parts in Table III to those found from the refinement using the $0kl$ reflections; y of S of TaS_2 was chosen to be equal to zero.

Final fractional atomic coordinates and thermal parameters (U_{eq} only) and site occupancy factors are given in Table III.[1] In all our calculations scattering factors were taken from Cromer and Mann (*14*). Anomalous dispersion factors are those given by Cromer and Liberman (*15*). All calculations were carried out on the CDC-Cyber 170/760 computer of the University of Groningen with the program packages XTAL (*16*) and EUCLID (*17*) (calculation of geometric data).

Description of the Structure

$(PbS)_{1.13}TaS_2$ is built of alternately puckered double layers of PbS and TaS_2 sandwiches alternating along c. The TaS_2 sandwiches are, apart from a distortion as discussed below, the same as those present in 2H–TaS_2. The relationship becomes visible by comparing the a and b axes of the TaS_2 part (Table I) with the orthohexagonal axes of 2H–TaS_2, $a = 3.314$ Å, $b = 12.097$ Å (*18*). On the basis of an orthohexagonal cell the space group is changed from $P6_3/mmc$ for 2H–TaS_2 to $Pm2c$ for the distorted structure. Due to the different type of stacking of TaS_2 sandwiches in 2H–TaS_2 and $(PbS)_{1.13}TaS_2$, the translational components of each element may differ for both compounds. It is thus found that the subsystem space group of the TaS_2 part, $Fm2m$, is compatible with the orthohexagonal space group of 2H–TaS_2.

Since the distortion (the deviation of b/a from $\sqrt{3}$) is small, the Ta–Ta distances, 3.326 Å (4×) and 3.305 Å (2×), differ only slightly; the average Ta–Ta distance, 3.319 Å, is the same as the Ta–Ta distance in 2H–TaS_2. The y coordinate of sulfur deviates considerably from $y = \frac{1}{3}$ for S in the orthohexagonal cell of 2H–TaS_2 which leads to Ta–S distances of 2.524(4) Å (2×) and 2.443(3) Å (4×) (Fig. 1). The average Ta–S bond length, 2.470 Å, is close to the Ta–S bond length, 2.468(2) Å, in 2H–TaS_2 (*18*).

The PbS sublattice of $(PbS)_{1.13}TaS_2$ consists of puckered double layers with lead atoms sticking outside the planes of sulfur.

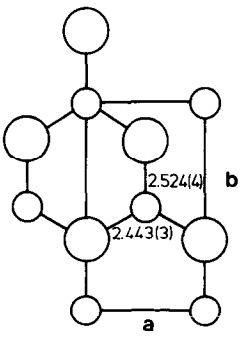

FIG. 1. Interatomic distances (in Å, e.s.d. in parentheses) in a TaS_2 sandwich projected along the c axis; small and large circles are Ta and S, respectively.

[1] See NAPS Document No. 04739 for 11 pages of supplementary material (F_o, F_c), anisotropic thermal parameters). Order from ASIS/NAPS. Microfiche Publications, P.O. Box 3513, Grand Central Station, New York, NY 10163. Remit in advance $4.00 for microfiche copy or for photocopy, $7.75 up to 20 pages plus $0.30 for each additional page. All orders must be prepaid.

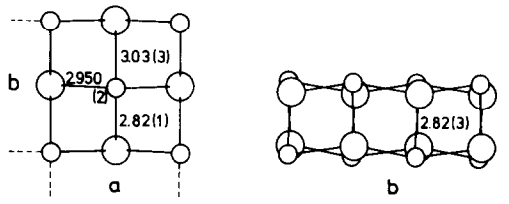

FIG. 2. Interatomic distances (in Å, e.s.d. in parentheses) in the upper half of a double layer of PbS. (a) Projected along [001]; (b) projected along [100]. Small and large circles are Pb and S, respectively.

Undistorted double layers with dimensions $5.936 \times 5.936 \times 2.968$ Å^3 can be made from solid PbS, with the latter having a NaCl-type structure, space group $Fm3m$, and $a =$ 5.936 Å (*19*). In order to accommodate TaS_2 sandwiches, such double layers are compressed to puckered double layers with the in-plane (*ab*) unit cell dimensions of 5.825×5.778 Å^2; along the commensurate *b* axes (5.778 Å) the PbS and TaS_2 units clamp each other. Perpendicular to the *ab* plane the distance between planes of lead atoms (the outer planes of atoms of the slab of PbS) is 3.281 Å which may be compared with 2.968 Å in the undistorted slab. The volume per unit PbS is hardly changed during the distortion, viz. from 26.15 Å^3 for PbS to 27.6 Å^3 for the distorted slab.

The coordination of Pb by S of the PbS unit is approximately square pyramidal, the bond to the apex S atom, approximately parallel the *c* axis, being 2.82(3) Å. Two of the four bonds approximately in the *ab* plane are equal, viz. those approximately along *a* (2.950(2) Å); the other two, approximately parallel to *b*, are 2.82(1) and 3.30(1) Å (Fig. 2). The average length of the latter four Pb–S bonds, 2.94 Å, is close to the Pb–S bond length in solid PbS.

Since lead atoms are in planes lying about 0.4 Å outside the planes of sulfur, the shortest interunit interactions are between sulfur atoms of TaS_2 and lead atoms. Compared to 2H–TaS_2, the van der Waals gap between neighboring sandwiches is replaced by a pseudo van der Waals gap with probably bonding interactions between lead atoms and sulfur atoms of TaS_2. Due to the incommensurate character of the structure along the *a* axes, the distances of Pb to three S atoms of TaS_2 vary (Fig. 3); together with the S atoms of the PbS slab the total number of sulfur atoms coordinating Pb becomes 7 or 8, depending on the actual position along the *a* axis in the misfit compound.

The stacking of PbS double layers and TaS_2 sandwiches is demonstrated in Fig. 4; sandwiches of the same type $(\frac{1}{2})c$ apart are displaced with respect of each other over $(\frac{1}{2})b$.

The structures of the subunits PbS and TaS_2 described above are modified due to their mutual modulation. One may assume the PbS lattice to be the strongest modulated because of the flexibility of the PbS slab. An indication for a stronger modulation of the PbS part is found in the temperature factors of the atoms, those of PbS being about five times larger than those of TaS_2 (Table III).

Superspace Group Description

The structures of the subsystems PbS and TaS_2 are both described in space group $Fm2m$. It was shown that $Fm2m$ is compatible with the orthohexagonal space group $Pm2c$ of 2H–TaS_2. The space group of orthorhombically distorted PbS, $Pmmm$, is a subgroup of $Fm3m$. That the PbS part does have a structure according to the space group $Fm2m$ is hereafter explained by the superspace group description of the symmetry.

As derived elsewhere (*20–22*), one higher dimensional space group can be defined, which characterizes the symmetry of the complete structure of an intergrowth compound. Following these procedures the four-dimensional superspace group $P^{Fm2m}_{1\,1\,1}$ (α 0 0) is obtained for $(PbS)_{1.13}TaS_2$.

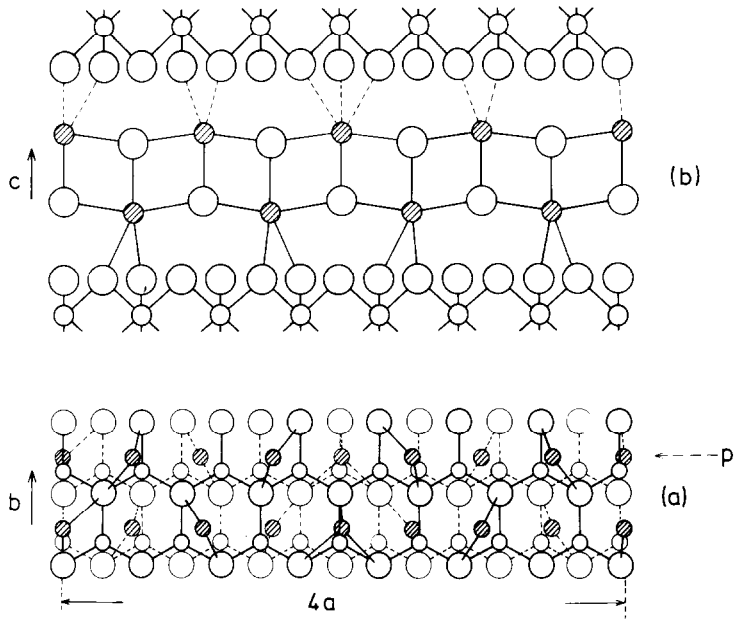

FIG. 3. (a) Projection of the structure of $(PbS)_{1.13}TaS_2$ along the [001] axes. Large and small open circles are S and Ta, respectively; Pb atoms are indicated by dashed circles. Along the misfit axes a length corresponding with four unit cells of the PbS part is indicated. Sulfur atoms of the PbS part are not drawn for the sake of clarity. (b) A projection along the [010] axes showing the coordination of Pb in one of the two PbS double layers. Only Pb atoms along the row indicated by p in (a) are shown. "Bonds" between Pb and S of TaS_2 are indicated by solid and dashed lines in (a) and (b).

The F-centering corresponds to the translations:

$$(\tfrac{1}{2},\ \tfrac{1}{2},\ 0,\ \tfrac{1}{2})$$
$$(\tfrac{1}{2},\ 0,\ \tfrac{1}{2},\ 0)$$
$$(0,\ \tfrac{1}{2},\ \tfrac{1}{2},\ \tfrac{1}{2}).$$

The four-dimensional reciprocal lattice projects onto the four vectors $\{\mathbf{a}_1^*, \mathbf{a}_2^*, \mathbf{a}_3^*, \mathbf{a}_4^*\}$ in physical, three-dimensional space. The reciprocal lattices of both subsystems are obtained from these as

$$\begin{bmatrix} \mathbf{a}_{\nu 1}^* \\ \mathbf{a}_{\nu 2}^* \\ \mathbf{a}_{\nu 3}^* \end{bmatrix} = Z^\nu \begin{bmatrix} \mathbf{a}_1^* \\ \mathbf{a}_2^* \\ \mathbf{a}_3^* \\ \mathbf{a}_4^* \end{bmatrix} \text{ with } Z^1$$

$$= \begin{bmatrix} 1 & 0 & 0 & 0 \\ 0 & 1 & 0 & 0 \\ 0 & 0 & 1 & 0 \end{bmatrix} \text{ and } Z^2 = \begin{bmatrix} 0 & 0 & 0 & 1 \\ 0 & 1 & 0 & 0 \\ 0 & 0 & 1 & 0 \end{bmatrix},$$

$\nu = 1$ and $\nu = 2$ corresponding to subsystems TaS_2 and PbS, respectively. $\mathbf{a}_4^* = \alpha \mathbf{a}_1^*$, with $\alpha = 0.5673$ as defined previously, gives the incommensurate ratio of the a axes in both subsystems.

The important feature for the present discussion is that the single superspace group uniquely defines the space group of each subsystem (*21, 22*). For the superspace group given here, together with the Z^ν-matrices, the subsystem space groups are obtained as given in Table I.

X-ray diffraction does not allow the determination of the presence or absence of a center of symmetry. Therefore, on the basis of the symmetry properties of the diffraction pattern only, the superspace group $P^{Fmmm}_{\bar{1}\bar{1}\bar{1}}$ (α 0 0) would also be possible. This would lead to the centrosymmetric subsystem space groups *Fmmm*. Because the TaS_2 component is acentric, it follows that the superspace group must be acentric.

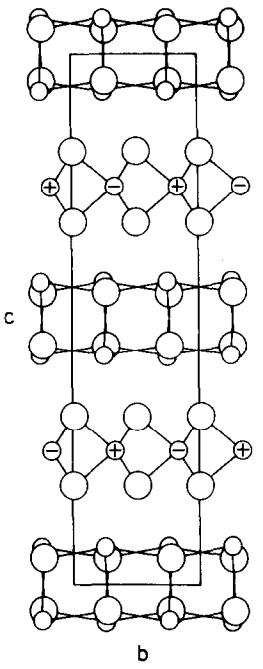

FIG. 4. The projection of the complete structure of $(PbS)_{1.13}TaS_2$ along the misfit axes. In order to demonstrate the *F*-centering of the TaS_2 lattice, tantalum atoms at $z = \frac{1}{4}$ and $z = \frac{3}{4}$ in the same plane parallel (100) have the same symbol (+ or −); atoms $(\frac{1}{2})a$ TaS_2 apart have different symbols.

This, in turn, leads to the space group *Fm2m* for the PbS subsystem, thus proving the latter to be noncentrosymmetric too.

Electrical Transport Properties and Magnetic Properties of $(PbS)_{1.13}TaS_2$

The in-plane resistivity ($\rho_\perp$) versus temperature curve (Fig. 5) shows a metallic type of conduction; the residual resistivity amounts to 10^{-7} Ω-m, the ratio $\rho_\perp$ (300 K)/$\rho_\perp$ (4 K) is 15. The resistivity along the *c* axis is also metallic (Fig. 6); the resistivity ratio $\rho_\parallel/\rho_\perp$ is 5×10^4. Such a large anisotropy in the conduction is also observed for $(SnS)_{1.17}NbS_2$ (*3*) and $(PbS)_{1.14}NbS_2$ (*4*). The Hall coefficient R_H as measured on two crystals is shown in Fig. 7; the differences between the two measurements is attributed to the uncertainty in the measurement of the thicknesses of the crystals (12 and 37 μm). R_H is in all cases positive and increases slightly below about 150 K with decreasing temperature. The number of holes calculated from the average R_H, 9×10^{-10} $m^3\ C^{-1}$ at 300 K, using $R_H = 1/(pe)$ (p is the number of holes, e the electron charge) amounts to 6.9×10^{27} m^{-3} which corre-

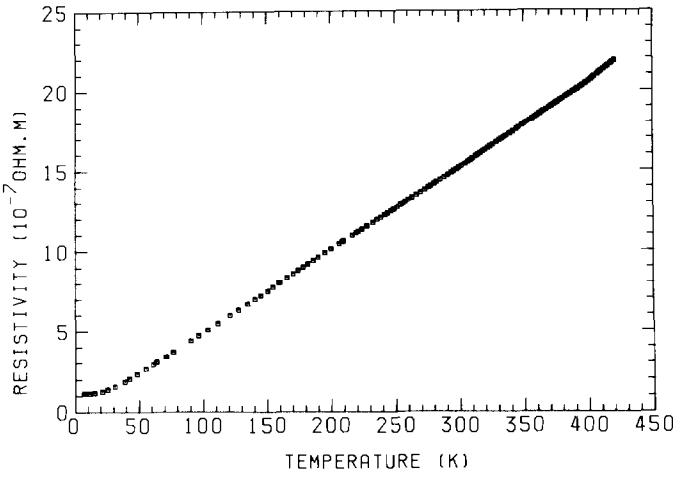

FIG. 5. The in-plane resistivity, $\rho_\perp$, versus temperature of $(PbS)_{1.13}TaS_2$.

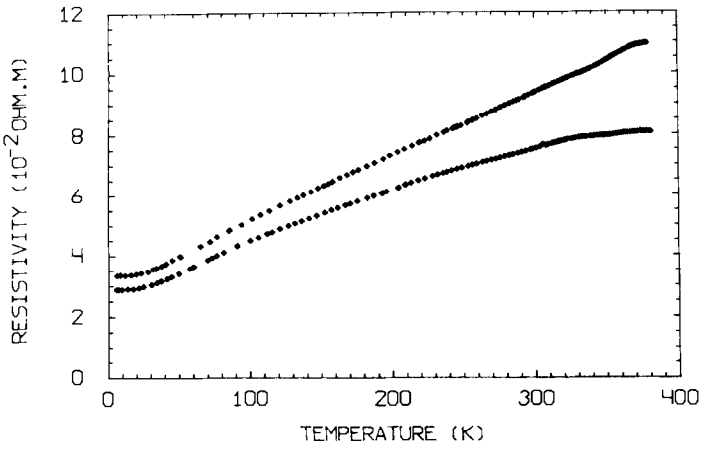

FIG. 6. The resistivity along the c axis, $\rho_{\parallel}$, versus temperature of $(PbS)_{1.13}TaS_2$ for two different crystals.

sponds to 0.8 hole/Ta. The Seebeck coefficient (Fig. 8) is negative from 300 K to about 50 K. The magnetic susceptibilities ($\chi_{\parallel}$ and $\chi_{\perp}$, not corrected for diamagnetism) of $(PbS)_{1.13}TaS_2$ are shown in Fig. 9. The anisotropy of χ, $\chi_{\parallel}$ being larger than $\chi_{\perp}$ was also observed in $(SnS)_{1.17}NbS_2$ (*3*) and intercalates Ag_xTaS_2 (*23*). The measured χ values of $(PbS)_{1.13}TaS_2$ are about 30% smaller than the corresponding values in $(PbS)_{1.14}NbS_2$; the difference may be due to a larger diamagnetic contribution in the Ta compound. A discussion of the anisotropy in χ is outside the scope of this paper.

A positive sign of R_H with values corresponding with less than a hole per transition metal and a negative Seebeck coefficient in the range 10–20 μV K^{-1} at 300 K was also observed for $(SnS)_{1.17}NbS_2$ (*3*), $(PbS)_{1.14}NbS_2$ (*4*), intercalates of silver in 2H–NbS_2 (*24*), and 2H–TaS_2 (*23*). The properties of the misfit layer compounds are therefore similar to those of intercalated 2H–NbS_2 and 2H–TaS_2. The 2H compounds are built

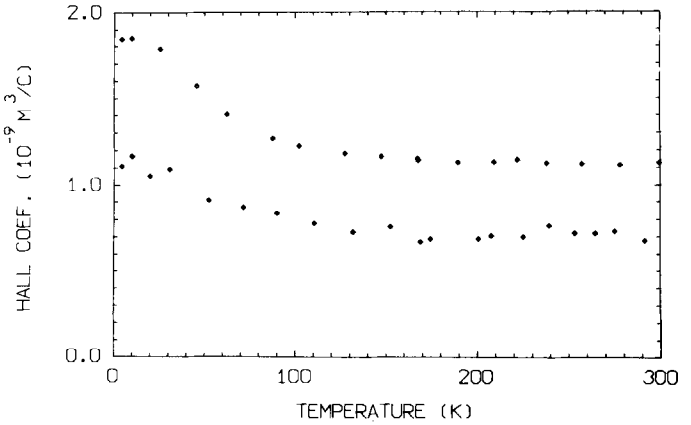

FIG. 7. The Hall coefficient, R_H, versus temperature of $(PbS)_{1.13}TaS_2$ for two different crystals.

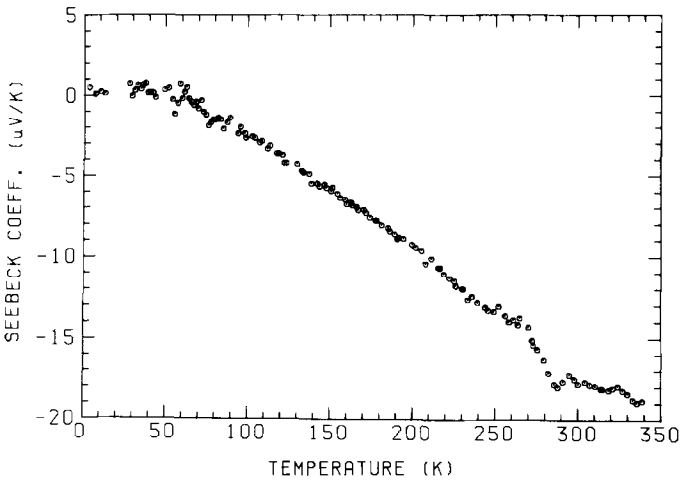

FIG. 8. The Seebeck coefficient of $(PbS)_{1.13}TaS_2$ versus temperature.

of NbS_2 and TaS_2 sandwiches with the transition metal in trigonal–prismatic coordination by sulfur. These compounds and also the corresponding selenides have been interesting subjects for experimental and theoretical studies due to their highly anisotropic physical properties and charge-density-wave (CDW) transitions resulting from the two-dimensional character of the Fermi surface. Band structure calculations (for a review, see Doni and Girlanda (*25*) and more recently those of Guo and Liang (*26*) and Dijkstra (*27*)) have shown that there is a valence band of mainly sulfur $3s$, $3p$ character overlapping (in Γ) a $5d_z2$ subband which is half-filled. The $5d_z2$ band hardly shows dispersion along the direction of the c^* axis. 2H–TaS_2 shows a CDW transition at 80 K; below the transition temperature an incommensurate distortion occurs

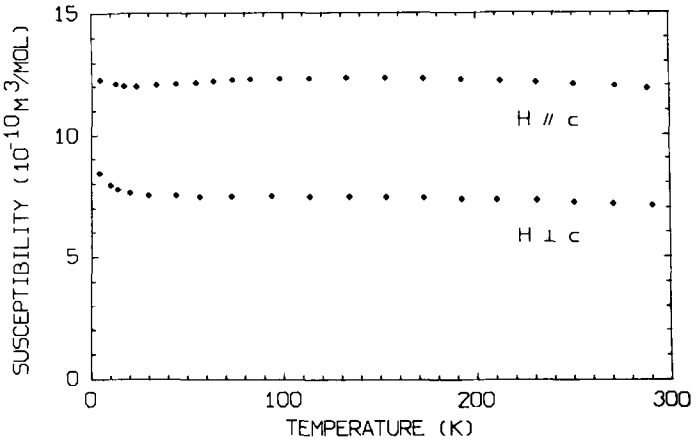

FIG. 9. The magnetic susceptibility $\chi_{\parallel}$ (upper curve) and $\chi_{\perp}$ (lower curve) versus temperature of $(PbS)_{1.13}TaS_2$ at a field of 0.875 T.

with hexagonal symmetry and wave vector $q = (1 - \delta)a^*/3$ ($\delta \approx 0$) (*28*). The properties of $(PbS)_{1.13}TaS_2$ as discussed above can be interpreted as those of intercalated 2H–TaS_2; the number of holes calculated from R_H, 0.8 per Ta, corresponds with a donation of 0.2 electron/Ta from the PbS part of the structure. The relatively large negative Seebeck coefficient indicates, compared to that of 2H–TaS_2, a change in the proportion of parts of the $5d_{z2}$ band with hole and electron character. The same was found for intercalates Ag_xTaS_2 (*23*). The donation of electrons is probably due to the $6s^2$ lone pair electrons of Pb, but the possibility of donation by valence band electrons of the PbS part cannot be excluded. The concept of a donor–acceptor-type interaction between the different structural units is supported by the properties of $(LaS)_{1.14}NbS_2$; this compound, isostructural with $(PbS)_{1.14}NbS_2$, shows a large donation in agreement with a preference for the valence state 3+ of La (*29*). The electrical transport and magnetic properties of $(PbS)_{1.13}TaS_2$ do not show anomalies which can be attributed to CDW transitions in the TaS_2 part of the structure. It may be remarked that in the misfit compound the TaS_2 lattice already has an orthorhombic distortion which makes a hexagonal CDW distortion impossible. Furthermore, the mutual interaction already gives a structurally induced modulation with wave vector $\alpha\mathbf{a}_1^*$. Van Maaren (*9*) and Schmidt *et al.* (*30*) found in a powder sample "$PbTaS_3$" superconductivity below 3.1 K. For 2H–TaS_2 superconductivity was reported below 0.65 K, T_c increasing with increasing pressure (*31*).

Acknowledgment

The research of S. van Smaalen has been made possible by financial support from the Royal Dutch Academy of Arts and Sciences (KNAW).

References

1. A. MEETSMA, G. A. WIEGERS, R. J. HAANGE, AND J. L. DE BOER, *Acta Crystallogr. Sect. A* **45,** 285, (1989).
2. S. KUYPERS, G. VAN TENDELOO, J. VAN LANDUYT, AND S. AMELINCKX, *Acta Crystallogr. Sect. A* **45,** 291, (1989).
3. G. A. WIEGERS, A. MEETSMA, R. J. HAANGE AND J. L. DE BOER, *Mater. Res. Bull.* **23,** 1551 (1988).
4. G. A. WIEGERS, A. MEETSMA, R. J. HAANGE, AND J. L. DE BOER, *in* "11th Intern. Symp. on the Reactivity of Solids," Princeton, USA (1988); *Solid State Ionics,* **32/33,** 183 (1989).
5. G. A. WIEGERS, S. VAN SMAALEN, A. MEETSMA, R. J. HAANGE, J. L. DE BOER, A. MEERSCHAUT, P. RABU, AND J. ROUXEL, to be published.
6. A. MEERSCHAUT, P. RABU, AND J. ROUXEL, *J. Solid State Chem.* **78,** 35 (1988).
7. W. STERZEL AND J. HORN, *Z. Anorg. Allg. Chem.* **376,** 254 (1970).
8. L. SCHMIDT, *Phys. Lett. A* **31,** 551 (1970).
9. M. H. VAN MAAREN, *Phys. Lett.* **40,** 353 (1972).
10. P. C. DONOHUE, *J. Solid State Chem.* **12,** 80 (1975).
11. S. KUYPERS, J. VAN LANDUYT, AND S. AMELINCKX, private communication.
12. L. E. MCCANDLISH, G. H. STOUT, AND L. C. ANDREWS, *Acta Crystallogr. Sect. A* **31,** 245 (1975).
13. A. L. SPEK, *in* "Proceedings, 8th Eur. Crystallogr. Meet.," Belgium (1983).
14. D. T. CROMER AND J. B. MANN, *Acta Crystallogr. Sect. A* **24,** 321 (1968).
15. D. T. CROMER AND D. LIBERMAN, *J. Chem. Phys.* **53,** 1891 (1970).
16. S. R. HALL AND J. M. STEWART, Eds. "XTAL2.2 User's Manual," Universities of Western Australia and Maryland (1987).
17. A. L. SPEK, "The EUCLID package," *in* "Computational Crystallography (D. Sayre, Ed.), p. 528, Oxford Univ. Press (Clarendon) London/New York (1982).
18. A. MEETSMA, G. A. WIEGERS, R. J. HAANGE, AND J. L. DE BOER, submitted for publication.
19. H. E. SWANSON AND R. K. FUYAT, U.S. National Bureau of Standards, Circ. 539, Vol. 2, p. 18 (1953).
20. A. JANNER AND T. JANSSEN, *Acta Crystallogr. Sect. A* **36,** 408 (1980).
21. S. VAN SMAALEN, submitted for publication.
22. S. VAN SMAALEN, *J. Phys: Condens. Matter* **1,** 1791 (1989).
23. A. DIEDERING, R. J. HAANGE AND G. A. WIEGERS, to be published.

24. H. J. M. BOUWMEESTER, Thesis, Groningen (1988).
25. E. DONI AND R. GIRLANDA, *in* "Electronic Structure and Electronic Transitions in Layered Materials" (Vincenzo Grasso, Ed.), p. 1, Reidel, Dordrecht, Holland (1986).
26. G. Y. GUO AND W. Y. LIANG, *J. Phys. C* **20,** 4315 (1987).
27. H. DIJKSTRA, Thesis, Groningen (1988).
28. A. H. THOMPSON, F. R. GAMBLE, AND R. F. KOEHLER, *Phys. Rev. B* **5,** 2811 (1972).
29. G. A. WIEGERS AND R. J. HAANGE, *J. Phys: Condens. Matter*, in press.
30. L. SCHMIDT, S. L. MCCARTHY, AND J. P. MAITA, *Solid State Commun.* **8,** 1513 (1970).
31. D. JEROME, C. BERTHIER, P. MOLINIE, AND J. ROUXEL, *J. Phys. Colloque* **C-4,** Suppl. aux No. 10, tome **37,** 125 (1976).